Available online at www.sciencedirect.com

ScienceDirect

IFAC Papers Online CONFERENCE PAPER ARCHIVE

IFAC PapersOnLine 55-27 (2022) 311–316

Control co-design of power take-off parameters for wave energy systems ⋆

Yerai Peña-Sanchez * **Demián García-Violini** **
John V. Ringwood ***

* *Euskal Herriko Unibertsitatea (EHU/UPV), Leioa, Bizkaia, España. (e-mail: yerai.pena@ehu.eus).*
** *CONICET & Universidad Nacional de Quilmes, Dept. de Ciencia y Tecnología, Roque Sáenz Pena 352, B1876, Buenos Aires, Argentina (corresponding author, e-mail: ddgv83@gmail.com)*
*** *Centre for Ocean Energy Research, Maynooth University, County Kildare, Ireland (e-mail: john.ringwood@eeng.nuim.ie)*

Abstract: A key component of wave energy converters (WECs), which determines the technical and economic performance of WECs, is the power take-off (PTO) system. This WEC subsystem converts the hydrodynamic excitation of the WEC into useful mechanical and, typically, electrical energy. It is well known that WEC control systems have the capability to significantly enhance the performance of WECs, but are limited in scope by the physical PTO displacement and force constraints. A variety of WEC control algorithms have the capacity to include the PTO constraints within the (constrained) optimal control formulation, delivering performance which takes maximum advantage of the available operational space, but avoiding exceedance of device/PTO specifications. However, little consideration is given to the interplay between the constraint levels and the maximum achievable performance. This paper examines, from an economic perspective, the trade-off between energy receipts and the capital cost of force and displacement constraints in a typical heaving point absorber WEC.

Keywords: Power take-off, constraints, wave energy, control co-design, energy maximisation.

1. INTRODUCTION

Despite the need for increasing amounts, and diversity, of renewable energy sources, wave energy has not yet reached commercial deployment. There are a number of reasons for this, not least the harsh ocean environment, the oscillating nature of the wave energy flux, relatively high force/velocity ratios, and the need for a dynamical mechanical system to survive extreme sea states. A complicating factor is the many and varied principles of operation of wave energy converters (WECs), exploiting a variety of wave characteristics, resulting in a lack of technology convergence. Ultimately, for commercial success, wave energy must achieve a Levelised Cost of Energy (LCoE) which is competitive with other renewable, and conventional, energy sources.

To this end, control technology has been identified as a potentially significant contributor to lowering the LCoE (Chang et al., 2018), while various optimisation studies have been carried out to identify the optimum WEC geometry (McCabe et al., 2010; Garcia-Teruel and Forehand, 2021; Guo and Ringwood, 2021). Significantly less attention has been paid to optimisation of the power take-off (PTO) system, with PTO optimisation studies typically focussing on the control settings (e.g. (Neshat et al., 2019)), rather than the specification of the PTO structure, or configuration. A useful review of WEC PTO systems can be found in (Ahamed et al., 2020).

Though the 'control co-design' label has only recently been employed to describe studies where optimisation is carried out in a 'control-aware' sense, the significance of the choice of control method, and/or tuning parameters, on various optimisation objectives and co-designed optimal parameters, has been the subject of a number of studies. For example, Garcia-Rosa and Ringwood (2015) show the interaction between control and optimal WEC geometry, while studies by Garcia-Rosa et al. (2015b) and Neshat et al. (2019) demonstrate the interaction between optimal array layout and control. However, the subject of PTO specification, in terms of either optimisation, or control co-design, has received comparatively little attention. One study, that does incorporate PTO constraints as a focal point, is that by Garcia-Rosa et al. (2015a), but with an emphasis on the effect of constraints on the optimal WEC geometry, rather than optimisation of the PTO specifications themselves. The study by Tan et al. (2022) is relevant in addressing PTO sizing, but uses a simple unconstrained control solution, which obscures the relationship between PTO size/capacity (constraints) and control performance. However, Tan et al. (2022) do incorporate a useful techno-economic treatment.

⋆ John Ringwood was supported by Science Foundation Ireland (SFI) through the MaREI Centre for Energy, Climate and Marine under Grant No. 12/RC/2302_P2. In addition, this project has received funding from the European Union's Horizon 2020 research and innovation programme under the Marie Sklodowska-Curie grant agreements N°101034297.

10.1016/j.ifacol.2022.10.531

Bacelli and Ringwood (2013) provides a mathematical/graphical platform for the investigation of the effect of PTO specifications on the optimal WEC control problem solution, using pseudospectral control as a basis, but their approach has the following drawbacks:

(a) Some conservatism is built into the constraint satisfaction analysis, due to to the need to convert from an infinity norm metric to a 2-norm metric, and
(b) The analysis is cumbersome for the panchromatic case.

Nevertheless, the analysis in (Bacelli and Ringwood, 2013) provides sufficient inspiration to consider how PTO specifications might be optimally configured. For example, Fig.1 shows the case for a vertical cylinder with diameter 10 m, draft 25 m and mass of 4.9 x 10^5 kg. The incident (monochromatic) sea is of 3 m amplitude, with a wave period of 11.4 s. PTO amplitude and force constraints are set at 3 m and 200 kN respectively. An intuitive feature of this representation is that the distance between force and position constraint circle centres, given by P_c, represents the magnitude of the wave excitation force, with a smaller P_c giving a larger viable control solution, represented by the shaded area. While the optimal unconstrained solution (in terms of P_1 and P_2) is given by $\bar{P}$, the optimal constrained solution is $\bar{P}_{constr}$. Clearly, from Fig.1, there is little advantage in increasing the position constraint, since there will be little movement in $\bar{P}_{constr}$ towards $\bar{P}$. However, in contrast, if the force constraint is relaxed, significant movement of $\bar{P}_{constr}$ towards $\bar{P}$ is achieved.

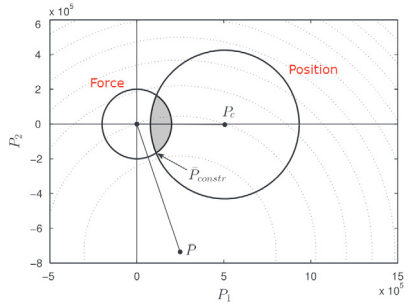

Fig. 1. Representation of a viable constrained control solution (adapted from (Bacelli and Ringwood, 2013)). Dotted lines show the energy contours, with a maximum at $\bar{P}$. P_1 and P_2 are the coefficients of *sin* and *cos* in the pseudospectral representation

This paper addresses the type of problem articulated in Fig.1, but from a overall system (economic) performance perspective. A similar (pseudospectral) controller to that of Bacelli and Ringwood (2013) is adopted, but a full panchromatic analysis is incorporated. While the intuitive graphical appeal of the representation in Fig.1 is lost, due to the necessary adoption of a numerical approach, the conservatism highlighted in (a) above is circumvented. A key objective, and challenge, is balancing the value of the extra energy captured against the capital cost of increases in displacement and/or force constraints.

The remainder of the paper is laid out as follows: The metrics and performance function, ultimately distilled to economic quantities and employed in the analysis, are described in Section 3. The optimal constrained pseudospectral control solution used is described briefly in Section 4.1.1, while the optimisation procedure is detailed in Section 4.2. An illustrative example of the PTO optimisation procedure is presented in Section 5 and conclusions are drawn in Section 6.

2. SYSTEM DESCRIPTION

For the sake of simplicity, a heaving point absorber (PA) WEC system [1], moving in one degree of freedom (DoF), is considered in this study. The relative motion of the device, measured from its equilibrium position, i.e. the still water level (SWL), is transformed into electric energy by means of the power-take-off (PTO) system, consisting of a linear generator, which is anchored to the sea bottom, as sketched in Fig. 2.

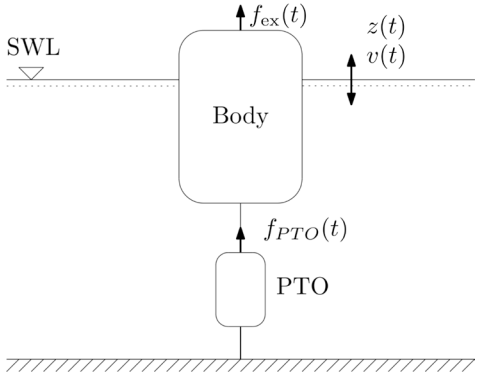

Fig. 2. Generic heaving point absorber, moving in one degree of freedom

2.1 Mathematical model

Using linear potential flow theory and Cummins' equation (Cummins, 1962), the motion of a single DoF WEC, as depicted in Fig. 2, can be described, for $t \in \mathbb{R}^+$, by

$$(m+m_\infty)\ddot{z}(t) = f_{\rm ex}(t) - f_{\rm PTO}(t) - k_{\rm h} z(t) - h_{\rm r} \star \dot{z}(t), \quad (1)$$

where the symbol $\star$ represents convolution, $f_{\rm ex}(t)$ is the wave excitation force, $f_{\rm h}(t)$ the hydrostatic restoring force, $m \in \mathbb{R}^+$ the mass of the device, $f_{\rm PTO}(t)$ the control force applied through the PTO system, $k_{\rm h}$ the hydrostatic stiffness, $h_{\rm r}(t)$ the radiation impulse response kernel, with $z(t)$, $\dot{z}(t)$, and, $\ddot{z}(t)$ representing the displacement, velocity, and acceleration of the WEC, respectively. In Eq. (1), $m_\infty = \lim_{\omega\to\infty} A_{\rm r}(\omega)$, with $A_{\rm r}(\omega)$ and $B_{\rm r}(\omega)$ the so-called radiation added-mass and damping, respectively, defined from Ogilvie's relations (Ogilvie, 1964).

2.2 PTO specification

In this study, the PTO system is assumed to be a direct drive linear generator, as depicted in Fig. 2. In addition, the PTO technology under consideration is assumed to have bidirectional power flow functionality, with the ability to apply both positive and negative control forces. Such

[1] Point absorber refers to a WEC system that extracts energy through the relative motion between a body that moves in response to wave forcing and fixed or immobile structures.

a PTO structure is widely considered throughout the literature for PA structures (Têtu, 2017). It is relatively easy to calculate the cost of these PTO systems, based on the required materials (see, for example, the studies presented by Tokat and Thiringer (2017) and Hodgins et al. (2011)). As explained in Section 3, the cost of the PTO system can be defined using its physical specification, such as maximum (or nominal) force, $F_{\max}$, and stroke, $S_{\max}$. Thus, the operational range of the complete WEC system, given by the PTO specifications, is as follows:

$$\begin{aligned} |z(t)| &\leq S_{\max}, \\ |f_{\text{PTO}}(t)| &\leq F_{\max}. \end{aligned} \tag{2}$$

3. ESTABLISHING A PERFORMANCE FUNCTION

As highlighted in Section 1, LCoE is the key metric which determines the economic viability, and profitability, of a wave energy project. To that end, LCoE is adopted as the fundamental objective, defined as:

$$\text{LCoE} = (\text{CapEx} + \text{OpEx})/(\text{Energy production}), \tag{3}$$

where CapEx ($) denotes capital expenditure and OpEx ($) denotes operational expenditure. Since energy production (EP) is measured in Wh, the units of LCoE are $/Wh. As a reference, recent LCoE estimates (Stehly et al., 2020) for wind energy are 38 $/MWh and 85 $/MWh, for onshore and (fixed bottom) offshore, respectively.

Variation in PTO constraints primarily affects CapEx and EP and, while some connections have been established between OpEx and control action (Nielsen et al., 2017) (which also relate to PTO constraints), for the purpose of the analysis in this paper, it will be assumed that OpEx is simply specified as a proportion of CapEx (OpEx = q·CapEx, $0 \leq q \leq 1$), which accounts for extra OpEx associated with a larger PTO system (more generous stroke and force constraints).

An assumption will also be made that PTO costs (C_{PTO}) are a fixed proportion of CapEx, estimated at 20% (Tan et al., 2022), so that $\text{CapEx} = \text{C}_{\text{PTO}} + \text{C}_{\text{WEC}} = 5\text{C}_{\text{PTO}}$, where C_{WEC} is the cost of the WEC system, excluding PTO. In order to calculate C_{PTO}, the 2MW linear generator presented by Hodgins et al. (2011) is considered as a reference. The PTO system is composed of two main physical parts: (1) the translator, the moving part that contains an iron core and the permanent magnets; and (2) the stator, the shaft on which the translator moves, containing the copper coils. The maximum force of the generator is defined by the length of the translator (L_{trans}) but, due to the modular structure of this type of PTO, several generators can be stacked in parallel to reduce L_{trans}. Thus, the cost of the PTO materials can be divided into stator (C_{stat}) and translator (C_{trans}) costs, defined as

$$\begin{aligned} \text{C}_{\text{trans}} &= F_{\max} \cdot \text{CoF} = n_{\text{gen}} \cdot F_{\text{trans}} \cdot \text{CoF} \\ \text{C}_{\text{stat}} &= n_{\text{gen}} \cdot (L_{\text{trans}} + S_{\max}) \cdot \text{CoS}, \end{aligned} \tag{4}$$

where n_{gen} is the number of generators stacked in parallel, F_{trans} the force capacity of each translator, and CoS and CoF are costs per unit length of stroke ($/m) and per unit force rating ($/N), respectively. Equation (5) provides an explicit relationship between the physical constraints (as implemented by the control system) and the translator and stator costs, which ultimately feed into LCoE. It should be noted that CoS and CoF can be calculated from the material requirements provided in (Hodgins et al., 2011). Thus, CoS and CoF can be straightforwardly obtained as a function of the unit costs of steel (C_{st}), copper (C_{cu}), magnets (C_{mg}), and epoxy resin (C_{ep}), as follows:

$$\begin{aligned} \text{CoF} &= \mu_{\text{st}}^{\text{trns}} + \mu_{\text{mg}}^{\text{trns}}, \\ \text{CoS} &= \mu_{\text{st}}^{\text{sttr}} + \mu_{\text{cu}}^{\text{sttr}} + \mu_{\text{ep}}^{\text{sttr}}, \end{aligned} \tag{5}$$

where the subscripts $\{\cdot\}_{\text{st}}$, $\{\cdot\}_{\text{mg}}$, $\{\cdot\}_{\text{cu}}$, and $\{\cdot\}_{\text{ep}}$ refer to the properties of steel, magnets, copper, and epoxy resin, respectively, and the superscripts $\{\cdot\}^{\text{trns}}$ and $\{\cdot\}^{\text{sttr}}$ refer to translator and stator properties, respectively. In Eq. (5), the right-hand side coefficients are defined as $\mu_{\{\cdot\}}^{\text{trns}} = \text{C}_{\{\cdot\}} \cdot m_{\{\cdot\}}/F^{\text{trns}}$ and $\mu_{\{\cdot\}}^{\text{sttr}} = \text{C}_{\{\cdot\}} \cdot m_{\{\cdot\}}/L^{\text{sttr}}$, with F^{trns} and L^{sttr} the translator force and stator length, respectively. Note that the parameters required in Eq. (5) can be obtained by scaling the magnitudes considered in the analysis presented by Hodgins et al. (2011). In this study, n_{gen} is selected for each $F_{\max}$ so that $L_{\text{trans}} < 10$m. Finally, C_{PTO} can be defined as

$$\text{C}_{\text{PTO}} = 2.5 \cdot (\text{C}_{\text{stat}} + \text{C}_{\text{trans}}) + \text{C}_{\text{elec}}, \tag{6}$$

where C_{elec} is the cost of the power electronics, which depends on the power rating of the PTO (Hodgins et al., 2011), and the factor of 2.5 is included to account for the manufacturing process. With this set of cost assumptions, (3) can now be recast as:

$$\text{LCoE} = \gamma \cdot \text{C}_{\text{PTO}}/\text{EP}, \tag{7}$$

where $\gamma = 5q$. However, since γ is a constant, the optimal $S_{\max}$ and $F_{\max}$ which minimise (7) are those that minimise:

$$\overline{\text{LCoE}} = \text{C}_{\text{PTO}}/\text{EP}, \tag{8}$$

with $\overline{\text{LCoE}}$ now adopted as the performance objective. We note that, in the paper, there is some inconsistency in the assumption of C_{WEC} being a proportion of C_{PTO}, since we will assume that, as the PTO changes, the size of the WEC body remains constant (allowing a single hydrodynamic model to be used). This inconsistency is sustained on the basis of focusing on the PTO control co-design problem, where changes in $S_{\max}$ and $F_{\max}$, considering a constrained pseudo-spectral control solution, affect both the numerator and denominator of (8).

4. CONTROL CO-DESIGN

4.1 Control solution

In this paper, a pseudospectral method is utilised to discretise the problem which approximates the states and control variables, in an N-dimensional vector space, with a linear combination of orthogonal basis functions, $\Phi = \{\phi_i\}_{i=1}^{N}$. The states and the control signal of the system are approximated as follows:

$$\begin{aligned} z_i(t) \approx z_i^N(t) &= \sum_{j=1}^{N} \phi_j(t) z_{ij} = \Phi(t)\hat{\text{z}}_i \\ f_{\text{PTO}}(t) \approx f_{\text{PTO}}^N(t) &= \sum_{j=1}^{N} \phi_j(t) \text{f}_{\text{PTO}j} = \Phi(t)\hat{\text{f}}_{\text{PTO}}, \end{aligned} \tag{9}$$

where weight vectors are grouped as $\hat{z}_i = [z_{i1} \cdots z_{iN}]^\intercal \in \mathbb{R}^N$, and $\hat{\text{f}}_{\text{PTO}} = [\text{f}_{\text{PTO}1}, \cdots \text{f}_{\text{PTO}N}]^\intercal \in \mathbb{R}^N$. These vectors are determined by forcing the projection of the residual functions over the set of test functions $\Psi = \{\psi_j\}_{j=1}^{N}$ to be

zero. Using this pseudospectral method, the approximation of the equation of motion results in the linear system:

$$\hat{\mathrm{v}} = G_o(\hat{\mathrm{f}}_{\mathrm{ex}} - \hat{\mathrm{f}}_{\mathrm{PTO}}), \tag{10}$$

where $\hat{\mathrm{v}} = [v_1\ v_2\ \cdots\ v_N]^\intercal$, where v, representing *velocity*, corresponds to the approximation of $\dot{z}(t)$, which can be obtained by a linear combination of the vectors $\hat{z}_i$, and $\hat{\mathrm{f}}_{\mathrm{PTO}}$. G_o, which represents the force-to-velocity system *model*, indicates the mapping between $\hat{\mathrm{f}}_{\mathrm{PTO}} + \hat{\mathrm{f}}_{\mathrm{ex}}$, which is the approximation of the input $f_i(t) = f_{\mathrm{PTO}}(t) + f_{ex}(t)$, and $\hat{\mathrm{v}}$. Additionally, in Eq. (10), $\hat{\mathrm{f}}_{\mathrm{ex}} = [\mathrm{f}_{\mathrm{ex}1}, \cdots\ \mathrm{f}_{\mathrm{ex}N}]^\intercal \in \mathbb{R}^n$, where the set $\{\mathrm{f}_{\mathrm{ex}i}\}_{i=1}^{N}$ contains the coefficients of the excitation force approximation on the basis $\Phi(\mathbf{T})$, i.e. $f_{ex}(t) = F_{ex}(\mathbf{T}) \approx \Phi(\mathbf{T})\hat{\mathrm{f}}_{\mathrm{ex}}$, with $\mathbf{T} = \{t_1, t_2, \ldots, t_M\}$, indicating an equally spaced time discretisation set with a sampling rate t_m. Thus, using $\Phi(\mathbf{T})$ and the time series related to each variable, e.g. $f_{ex}(t)$, f_{PTO}, $v(t)$, etc, each corresponding pseudospectral approximation is obtained. Thus, coefficients of the excitation force, $\hat{\mathrm{e}}$, are computed as follows:

$$\hat{\mathrm{f}}_{\mathrm{ex}} = (\Phi(\mathbf{T})^\intercal \Phi(\mathbf{T}))^{-1} \Phi(\mathbf{T})^T F_{ex}(\mathbf{T}). \tag{11}$$

The basis functions are chosen such that G_o satisfies

$$G_o = \bigoplus_{k=1}^{N/2} \begin{bmatrix} \mathcal{R}_k^o & \mathcal{I}_k^o \\ -\mathcal{I}_k^o & \mathcal{R}_k^o \end{bmatrix}, \tag{12}$$

where

$$\mathcal{R}_k^o = \mathbb{R}e\{g_o(j\omega_k)\},\ \mathcal{I}_k^o = \mathbb{I}m\{g_o(j\omega_k)\}, \tag{13}$$

with $\mathcal{R}_k^o$, $\mathcal{I}_k^o \in \mathbb{R}$, and $g_o(j\omega_k)$ representing the nominal frequency response of the system, at frequencies ω_k. Additionally, $G_o \in \mathbb{R}^n$ is a block diagonal matrix and the symbol $\bigoplus$ denotes the direct sum of n matrices, i.e. $\bigoplus_{i=1}^{n} A_i = diag\{A_1,\ A_2,\ \cdots, A_n\}$.

Control Problem: The control objective for the WEC system is to maximise the total absorbed energy. For a WEC system, which is subject to an external excitation force $f_{ex}(t)$ and is controlled via a control force $u(t)$, the total absorbed energy over the interval $[0\ T]$, is computed as:

$$E = -\int_0^T P dt = -\int_0^T \dot{z}^\intercal(t) f_{\mathrm{PTO}}(t) dt, \tag{14}$$

where E is the absorbed energy (in J), P the instantaneous power (in W), and $f_{\mathrm{PTO}}(t)$ and $\dot{z}(t)$ are the control force and the device velocity (in N and m/s), respectively, both introduced in Eq (1). The interested reader is referred to (Falnes, 2002) for a detailed derivation of Eq. (14). The optimal control problem consists of obtaining the PTO control force $f_{\mathrm{PTO}}(t)$ that maximizes the objective function in Eq (14), subject to the equation of motion. Due to orthogonality of the basis functions ϕ_j, the application of pseudospectral approximations to the objective function in Eq. (14) results in:

$$J_N = \int_0^T \hat{\mathrm{f}}_{\mathrm{PTO}}^\intercal \Phi^\intercal(t) \Phi(t) \hat{\mathrm{v}} = -\frac{T}{2} \hat{\mathrm{f}}_{\mathrm{PTO}}^\intercal \hat{\mathrm{v}}, \tag{15}$$

transforming the integral relationship of Eq. (14) into an algebraic equation.

Optimal solution: Using speudospectral methods, the control problem for WEC systems can now be described as follows:

$$\begin{aligned} \hat{\mathrm{f}}_{\mathrm{PTO}}^\star \leftarrow \max_{\hat{\mathrm{f}}_{\mathrm{PTO}} \in \mathbb{R}^N} \leftarrow\ & J_N \\ \text{subject to:}\ & \mathcal{C} \end{aligned}, \tag{16}$$

which is a finite dimension quadratic optimisation problem, where the optimisation is carried out solely over the control variable $\hat{\mathrm{u}}$, and $\mathcal{C}$ represents a set of constraints arising from the physical limitations of the WEC system. In particular, for the application case in Section 5, the maximum PTO force (F_{max}) and stroke length (S_{max}), are considered in the definition of $\mathcal{C}$. In general, to fulfil the specified set of constraints, given in this study in Eq. (2), one possible approach is to enforce the constraints only at a set of specified time instants, referred to as collocation points, defined in a vector $\mathbf{T}_c = [t_1, t_2, \ldots t_{N_c}]$. Thus, for this study, the set of constraints in Eq. (2) can be translated into an inequality constraint, as follows

$$\mathcal{C} := \begin{bmatrix} A_{\mathrm{PTO}} \\ A_Z \end{bmatrix} \hat{\mathrm{f}}_{\mathrm{PTO}}^\intercal \leq \begin{bmatrix} b_{\mathrm{PTO}} \\ b_{\mathrm{Z}} \end{bmatrix}, \tag{17}$$

where

$$\begin{aligned} A_{\mathrm{PTO}} &= \begin{bmatrix} \Phi(\mathbf{T}_c) \\ -\Phi(\mathbf{T}_c) \end{bmatrix}, \quad A_Z = \begin{bmatrix} \Phi(\mathbf{T}_c) G_o \\ -\Phi(\mathbf{T}_c) G_o \end{bmatrix}, \\ b_{\mathrm{PTO}} &= \begin{bmatrix} F_{\max} \hat{\mathbf{1}} \\ F_{\max} \hat{\mathbf{1}} \end{bmatrix}, \quad b_Z = \begin{bmatrix} S_{\max} \hat{\mathbf{1}} - \Phi(\mathbf{T}_c) \hat{\mathrm{f}}_{\mathrm{ex}} \\ S_{\max} \hat{\mathbf{1}} + \Phi(\mathbf{T}_c) \hat{\mathrm{f}}_{\mathrm{ex}} \end{bmatrix}, \end{aligned} \tag{18}$$

with $\hat{\mathbf{1}} \in \mathbb{R}^{2N_c \times 1}$ a column vector of ones. The problem stated in Eq. (16) can be solved with standard numerical toolboxes.

4.2 PTO specification optimisation procedure

The optimisation problem considered for the PTO co-design methodology proposed in this study, can be expressed as follows [2]:

$$\begin{aligned} \begin{bmatrix} F_{\max}^\star \\ S_{\max}^\star \end{bmatrix}^\intercal \leftarrow \min_{[F_{\max},\, S_{\max}] \in \mathbb{R}^2}\ & \overline{\mathrm{LCoE}} \\ \text{subject to:}\ & \text{Solve Eq. (16)} \\ & F_{\max} \in \left[F_{\max}^\ell\, F_{\max}^u\right], \\ & S_{\max} \in \left[S_{\max}^\ell,\, S_{\max}^u\right], \end{aligned} \tag{19}$$

where the superscripts ℓ and u indicate the considered upper and lower bounds for the constraint analysis, respectively. In this study, the optimisation problem introduced in Eq. (19) is solved using a brute-force search methodology. However, it must be noted that the problem stated in Eq. (19) can be addressed using, for example, multi-objective optimisation routines (Miettinen, 2012), or other numerical search methods, as applied in a number of co-design studies. However, the use of a brute-force method, which amounts to a parametric study, has certain advantages since, by examining the full landscape of possibilities, it explicitly evidences the interplay between parameters, which gives further insight into the problem and solution domains.

5. ILLUSTRATIVE EXAMPLE

For the illustrative example of this section, a heaving 10 m diameter and 25 m draft cylinder, similar to that mentioned in Section 1 (Bacelli and Ringwood, 2013), is

[2] Note that the total absorbed energy, indicated in Eq. (14), implicitly affects the value of $\overline{\mathrm{LCoE}}$ in (8) via the control solution of (16).

selected. It is important to note that, due to the cylindrical structure of the considered WEC system, the 25 m draft length, and the stroke range under study, the linearity assumption considered for the analysis provides a consistent framework. While a more comprehensive analysis of the resulting performance would include a nonlinear dynamical characterisation of the system, the considered framework permits a reasonably accurate assessment of the final performance. A more complete performance assessment, considering a nonlinear description of the system, is beyond the scope of this preliminary study. The analysis of the PTO force and stroke constraints, as introduced in Eq. (19), is carried out using $F^{\ell}_{\max} = 5 \cdot 10^4$ N, $F^{u}_{\max} = 5 \cdot 10^8$ N, $S^{\ell}_{\max} = 5$ m, and $S^{u}_{\max} = 50$ m. In order to compute $\overline{\text{LCoE}}$ for each PTO configuration as shown in Eq. (8), the energy produced by the WEC must be estimated. To this end, it is assumed that the life expectancy of the device is 20 years and that there is no interruption to power production over the lifetime of the device (for simplicity). Also, again for the sake of simplicity, a single panchromatic sea state is considered in this study. However, a more comprehensive treatment would utilise a scatter plot (Barstow et al., 2008) to give a statistical description of the sea conditions at a particular wave energy site. The waves are synthesised using filtered white noise (Tucker et al., 1984), based on a JONSWAP spectrum (Hasselmann, 1973), and the considered parameters are a significant wave height $H_s = 6.5$ m, peak period $T_p = 10$ s, and steepness factor $\gamma = 3.3$. Thus, both the WEC structure and the sea-state considered in this study, have been also used by Bacelli and Ringwood (2013). To produce statistically consistent results, 14 realisations of the considered sea-state are used. Each simulation is performed over 200 s, which represents 20 times the peak period of the considered sea-state. The optimisation problem for computation of the optimal control force, expressed in Eq. (16), is solved via an interior-point method, using the Optimisation Toolbox in Matlab R2021.

To calculate C_{PTO}, the material cost coefficients specified in (Tokat and Thiringer, 2017; Hodgins et al., 2011) are considered, and listed in Table 1. Using the material cost information provided in Table 1, and considering the linear generator introduced by Hodgins et al. (2011) as a reference, values of CoS=$1.48 \cdot 10^3$\$/m and CoF=0.1656\$/N are obtained. Thus, the total PTO system costs, as defined in Eq. (6), for the different stroke and force constraint ranges, are depicted in Fig. 3. It can be noted, from Fig.3, that a significantly nonlinear relationship between the physical constraints and C_{PTO} exists, even for the relatively simplistic set of cost relationships adopted in Section 3. It can be noted in Fig. 3 that, for the considered stroke and force constraint bounds, the C_{PTO} increase along the $\text{F}_{\max}$ axis is significantly greater than that along the $\text{S}_{\max}$ axis, i.e. the cost of PTO force capacity is significant.

Table 1. Cost coefficients of the PTO materials.

Material costs coefficients			
C_{st} [\$/kg]	C_{cu} [\$/kg]	C_{mg} [\$/kg]	C_{ep} [\$/kg]
3.6	16.7	27.1	113.9

Fig. 4 shows the obtained $\overline{\text{LCoE}}$ values for the considered $\text{S}_{\max}$ and $\text{F}_{\max}$ combinations, with the minimum of $\overline{\text{LCoE}}$, denoted as $\text{LCoE}^{\star}$, marked with a red dot. $\text{LCoE}^{\star}$ is approximately 49.6\$/MW, obtained for $\text{S}^{\star}_{\max} \approx 17$m and $\text{F}^{\star}_{\max} \approx 2.59 \cdot 10^5$N. It is noticeable that $\overline{\text{LCoE}}$ increases rapidly when moving away from the optimal PTO configuration, which emphasises the importance that choosing the correct PTO constraints has on the economic viability of a WEC. To contextualise the results in Fig 4, the resulting power in the unconstrained scenario, for the considered sea state, is 6.036 MW, which can be considered as a benchmark. However, it can be noted from the results in Fig. 4 that, in the unconstrained case (i.e. sufficiently large $S_{\max}$ and $F_{\max}$), the value of $\overline{\text{LCoE}}$ makes the WEC system commercially unviable.

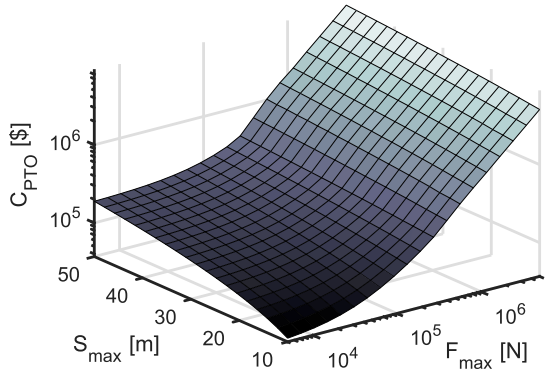

Fig. 3. Cost of the PTO system for the considered displacement and force constraints.

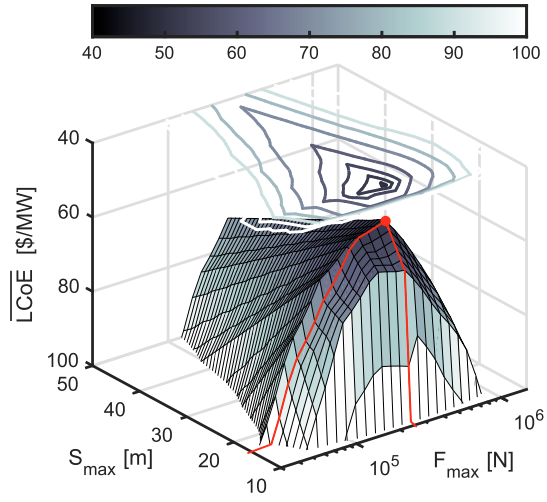

Fig. 4. Obtained $\overline{\text{LCoE}}$ for different $\text{S}_{\max}$ and $\text{F}_{\max}$. Note that an inverted vertical axis is used for clarity of presentation.

By way of example, Fig. 5 shows the motion of the device, along with both f_{PTO} and f_{ex}, for a given sea state realisation using the obtained optimal $\text{S}^{\star}_{\max}$ and $\text{F}^{\star}_{\max}$, confirming the capability of the controller in strictly adhering to the specified physical constraints.

6. CONCLUSION

The paper examines the relationship between the achievable force and stroke PTO constraint landscape, within which the control problem has a feasible solution, and the cost of achieving those constraints, closely related to

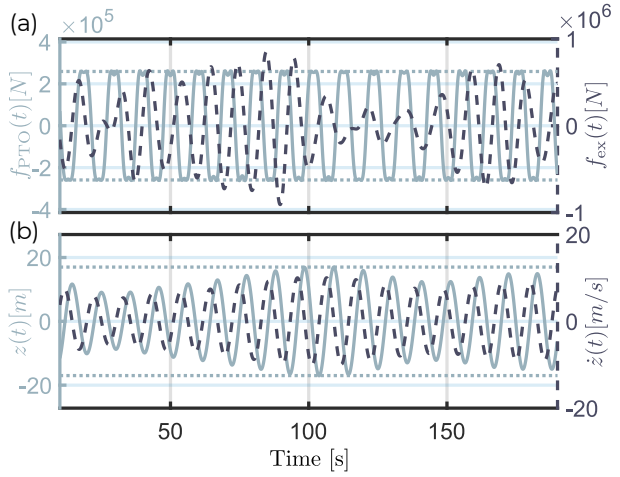

Fig. 5. (a) Time traces for f_{PTO} (solid line) and f_{ex} (dashed line). (b) Time traces for $z(t)$ (solid line) and $\dot{z}(t)$ (dashed line). The considered limits $S_{\max}$ and $F_{\max}$ are indicated in each corresponding plot using dotted lines.

LCoE. To the best of the authors' knowledge, this is the first time that such a study has been undertaken. Since a number of simplifying assumptions have been used to relate LCoE to $S_{\max}$ and $F_{\max}$, the process could be enhanced by a more comprehensive economic model. However, even with such simplifying assumptions, the relationship between the PTO cost and ($S_{\max}$, $F_{\max}$) is nonlinear, with a resulting nontrivial problem in optimising LCoE (or $\overline{\mathrm{LCoE}}$). The use of a brute-force approach results in a parametric study which reveals the full PTO configuration landscape, showing a relatively high sensitivity of LCoE to ($S_{\max}$, $F_{\max}$). This indicates the need to carefully choose the PTO characteristics to maximise the economic performance of a wave energy project. The presented control co-design procedure is not limited to the pseudospectral control method employed; rather, any WEC control philosophy which calculates an optimal (hard) constrained solution could be included. Finally, a more comprehensive analysis would employ a statistical scatter plot representation of the sea conditions at a chosen wave energy site.

REFERENCES

Ahamed, R., McKee, K., and Howard, I. (2020). Advancements of wave energy converters based on power take off (pto) systems: A review. *Ocean Engineering*, 204, 107248.

Bacelli, G. and Ringwood, J.V. (2013). A geometric tool for the analysis of position and force constraints in wave energy converters. *Ocean Engineering*, 65, 10–18.

Barstow, S., Mørk, G., Mollison, D., and Cruz, J. (2008). The wave energy resource. In *Ocean Wave Energy*, 93–132. Springer.

Chang, G., Jones, C.A., Roberts, J.D., and Neary, V.S. (2018). A comprehensive evaluation of factors affecting the levelized cost of wave energy conversion projects. *Renewable Energy*, 127, 344–354.

Cummins, W.E. (1962). The impulse response function and ship motions. *Schiffstechnik*, 47, 101–109.

Falnes, J. (2002). *Ocean waves and oscillating systems: linear interactions including wave-energy extraction*. Cambridge Univ. Press.

Garcia-Rosa, P.B., Bacelli, G., and Ringwood, J.V. (2015a). Control-informed geometric optimization of wave energy converters: The impact of device motion and force constraints. *Energies*, 8(12), 13672–13687.

Garcia-Rosa, P.B., Bacelli, G., and Ringwood, J.V. (2015b). Control-informed optimal array layout for wave farms. *IEEE Transactions on Sustainable Energy*, 6(2), 575–582.

Garcia-Rosa, P.B. and Ringwood, J.V. (2015). On the sensitivity of optimal wave energy device geometry to the energy maximizing control system. *IEEE Transactions on Sustainable Energy*, 7(1), 419–426.

Garcia-Teruel, A. and Forehand, D. (2021). A review of geometry optimisation of wave energy converters. *Renewable and Sustainable Energy Reviews*, 139, 110593.

Guo, B. and Ringwood, J.V. (2021). Geometric optimisation of wave energy conversion devices: A survey. *Applied Energy*, 297, 117100.

Hasselmann, K. (1973). Measurements of wind wave growth and swell decay during the Joint North Sea Wave Project (JONSWAP). *Deutches Hydrographisches Institut*, 8, 95.

Hodgins, N., Keysan, O., McDonald, A.S., and Mueller, M.A. (2011). Design and testing of a linear generator for wave-energy applications. *IEEE Transactions on Industrial Electronics*, 59(5), 2094–2103.

McCabe, A., Aggidis, G., and Widden, M. (2010). Optimizing the shape of a surge-and-pitch wave energy collector using a genetic algorithm. *Renewable Energy*, 35(12), 2767–2775.

Miettinen, K. (2012). *Nonlinear multiobjective optimization*, volume 12. Springer Science & Business Media.

Neshat, M., Alexander, B., Sergiienko, N.Y., and Wagner, M. (2019). A hybrid evolutionary algorithm framework for optimising power take off and placements of wave energy converters. In *Proceedings of the Genetic and Evolutionary Computation Conference*, 1293–1301.

Nielsen, K.M., Pedersen, T.S., Andersen, P., and Ambühl, S. (2017). Optimizing control of wave energy converter with losses and fatigue in power take off. *IFAC-PapersOnLine*, 50(1), 14680–14685.

Ogilvie, T.F. (1964). Recent progress toward the understanding and prediction of ship motions. In *5th Symposium on naval hydrodynamics*, volume 1, 2–5. Bergen, Norway.

Stehly, T., Beiter, P., and Duffy, P. (2020). 2019 cost of wind energy review. Technical report, NREL, USA.

Tan, J., Polinder, H., Laguna, A.J., and Miedema, S. (2022). The application of the spectral domain modeling to the power take-off sizing of heaving wave energy converters. *Applied Ocean Research*, 122, 103110.

Têtu, A. (2017). Power take-off systems for wecs. In *Handbook of ocean wave energy*, 203–220. Springer, Cham.

Tokat, P. and Thiringer, T. (2017). Sizing of ipm generator for a single point absorber type wave energy converter. *IEEE Transactions on Energy Conversion*, 33(1), 10–19.

Tucker, M., Challenor, P.G., and Carter, D. (1984). Numerical simulation of a random sea: a common error and its effect upon wave group statistics. *Applied Ocean Research*, 6(2), 118–122.